Evaluation of Reference Model for Thermal Energy System Based on Machine Learning Algorithm

Minsung Kim
School of Energy Systems Engineering
Chung-Ang University
Seoul, Republic of Korea
email: minsungk@cau.ac.kr

Young-Soo Lee
Thermal Energy System Laboratory
Korea Institute of Energy Research
Daejeon, Republic of Korea
email: yslee@kier.re.kr

***Abstract*—Since thermal energy systems are comprised in a number of heat exchangers and fluid machinery, it is complicated and time consuming to analyze the systems mathematically. For heat pumps, a number of mathematical studies have been carried out to identify their operating status; however, accurate models are very difficult to develop due to numerous cases of different installation and operating conditions. As an alternative way to estimate the performance, a methodology using machine learning algorithm is introduced to develop a reference model. A steady-state detector with a simple low pass filter is applied to filter signals. Once steady state of the system is identified, the real-time measurements are collected to train the system model. From the study, the semi-expert based learning algorithm is effective to develop reference models of heat pump systems.**

Keywords-Thermal energy systems; Steady state; Machine learning; Fault detection and diagnosis.

I. INTRODUCTION

An increasing emphasis on energy saving and environmental conservation requires air conditioners and heat pumps to be highly efficient. In the first place, a variety of research and development on a cycle as well as its basic components have been performed to increase overall efficiency of heat pump systems. A survey of over 55,000 residential and commercial units found the refrigerant charge to be incorrect in more than 60 % of the systems [1]. Another independent survey of 1500 rooftop units showed that the average efficiency was only 80 % of the expected value, primarily due to improper refrigerant charge [2]. To this end, various technologies were reported to analyze the performance of heat pump systems including the function of fault detection and diagnosis [3]-[5].

The development of Fault Detection and Diagnosis (FDD) method includes a laboratory phase during which fault-free and faulty operations are mapped, and an analytical phase during which FDD algorithms are formulated. These techniques typically produce the reference data under the combinations of test conditions which were modulated in laboratory. However, it is very difficult to produce a set of reference data in field systems since the configurations of heat pumps are different. Even in the cases of previous studies performed in laboratories, great efforts are taken to build up reference experiment. From this end, a machine learning algorithm is introduced in this study to produce the reference model out of field operating data of a heat pump system. The reference model was generated at steady states. To generate machine learning procedure, two environmental chambers were programmed randomly reflecting field environment. From the study, a reference model of the heat pump system was obtained very handful and convenient way with an acceptable accuracy.

In this paper, a reference model was described for a heat pump system in section II and the model was statistically evaluated in section III. From the analysis, methodological approach was introduced for a machine learning in section IV.

II. STEADY STATE MODELING OF HEAT PUMPS

In this study, the FDD process was envisioned to be performed every time the system is in steady state. The concept of the steady-state detector originates from noise filter theory. When a system is not steady, thermodynamic system parameters are highly unstable. The variance, or standard deviation, of important parameters is typically utilized to indicate the statistical spread within the data distribution and can be used to characterize random variation of the measured signals.

A. Determination of characteristic variables

Typical temperature-entropy (*T-s*) diagram presenting a vapor compression cycle is plotted in Figure 1. Since temperature measurements are most suitable and costly effective, the 7 parameters were selected as characteristic variables. The selected seven features are: Evaporator exit refrigerant saturation temperature (T_E), evaporator exit refrigerant superheat (T_{sh}), condenser inlet refrigerant saturation temperature (T_C), compressor discharge refrigerant temperature (T_D), condenser exit liquid line refrigerant subcooled temperature (T_{sc}), evaporator air temperature change (ΔT_{EA}), and condenser air temperature change (ΔT_{CA}).

As inputs of the characteristic variables, three parameters were chosen; outdoor dry-bulb temperature (T_{OD}), indoor dry-bulb temperature (T_{ID}), and indoor dew point temperature (T_{IDP}). The reference model was developed with the 3 independent variables and the 7 dependent variables.

The temperature sensors are T-type thermocouples with 0.5°C of uncertainties. Although the above features are limited only by 7 points and the temperature sensors are with

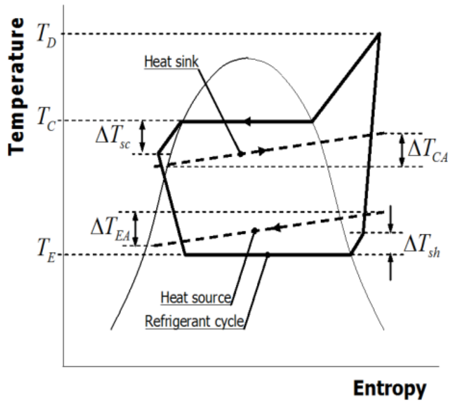

Figure 1. *T-s* diagram of a vapor compression heat pump system

relatively large uncertainties, limited measurements are maintained to reflect field measurements.

The variables were regressed upon the generated from the experimental database. Equations were in the form of the 1st, 2nd, and 3rd order Multivariate Polynomial Regression (MPR) models. After the residuals of the characteristic parameters can be obtained from the system, FDD process identifies defects of the system by analyzing the residuals with thresholds value which determine the system status.

B. *Determination of characteristic variables*

According to the features defined above, the variables were regressed upon the database generated from the experiments. Equations below show a general form of the regressed equations for the i^{th} feature (or i^{th} dependent variable) as the 2^{nd} and 3^{rd} order MPR models.

$$\begin{aligned}\phi_i^{(2)} &= a_0 + a_1 T_{\text{OD}} + a_2 T_{\text{ID}} + a_3 T_{\text{IDP}} + a_4 {T_{\text{OD}}}^2 + a_5 {T_{\text{ID}}}^2 \\ &\quad + a_6 {T_{\text{IDP}}}^2 + a_7 T_{\text{OD}} T_{\text{ID}} + a_8 T_{\text{ID}} T_{\text{IDP}} + a_9 T_{\text{IDP}} T_{\text{OD}}\end{aligned} \tag{1}$$

$$\begin{aligned}\phi_i^{(3)} &= \phi_i^{(2)} + a_{10} {T_{\text{OD}}}^3 + a_{11} {T_{\text{ID}}}^3 + a_{12} {T_{\text{IDP}}}^3 + a_{13} T_{\text{OD}} T_{\text{ID}} T_{\text{IDP}} \\ &\quad + a_{14} {T_{\text{OD}}}^2 T_{\text{ID}} + a_{15} {T_{\text{OD}}}^2 T_{\text{IDP}} + a_{16} {T_{\text{ID}}}^2 T_{\text{OD}} + a_{17} {T_{\text{ID}}}^2 T_{\text{IDP}} \\ &\quad + a_{18} {T_{\text{IDP}}}^2 T_{\text{OD}} + a_{19} {T_{\text{IDP}}}^2 T_{\text{ID}}\end{aligned} \tag{2}$$

From the above equations, residuals of the characteristic parameters can be obtained. After the residuals are measured from the system, FDD process identifies defects of the system by analyzing the residuals with thresholds value which determine the system status.

C. *Machine learning process*

Once the steady-state is identified, key performance parameters were evaluated from the references. We validated measured Coefficient of Performance (COP) – an efficiency parameter – and heating/cooling capacity by comparing the manufacturer's data. If there is no manufacturer's data, the system with no fault incorporated was pre-operated to evaluate the reference operation of the system. Once the key parameters are evaluated as no fault operation, the measured features are used to train the reference module. When the COP or heating capacity is out of range from the reference value, the system is assigned to be at a faulty status and FDD procedure is carried out.

III. VALIDATION OF THE MACHINE LEARNING BASED REFERENCE MODEL

To determine a realistic value of the threshold, validation of the measurements is mandatory. We counted three uncertainties of steady state, repeatability, and model itself. Naturally, the system measurements have uncertainties due to sensors – mostly thermocouples – and due to lack of measurement repeatability. Once the uncertainties by sensors will be evaluated, model uncertainty will be evaluated by the sensor uncertainties. In this section, the uncertainties are evaluated in statistical values.

A. *Uncertainties due to steady-state variation and lack of measurement repeatability*

The uncertainty of a thermocouple may come from measurement noise and drift. Considering that the measurement noise behaves like zero-mean white noise, its natural variation can be characterized closely by the steady-state standard deviation, $\sigma_{i,\text{SS}}$. Thermocouple drift is the measurement bias that varies over longer time periods than noise. However, the thermocouple drift can be regarded as negligible in this research since the same built-in sensors are used for model development and application to the tested system for FDD, thus their bias has been considered in the reference model measurements for this investigation. To observe the repeatability of the system measurements, we analyzed 38 repetitive tests of Kim et al. (2006) [6]. The feature standard deviations from repeatability tests, $\sigma_{i,\text{Repeat}}$, are listed in Table 1. In the table, the measurement uncertainties were provided due to by due to steady-state variation, $\sigma_{i,\text{SS}}$, and due to by the variation from test-to-test (measurement repeatability), $\sigma_{i,\text{Repeat}}$, for similar test conditions. These two values will be used to calculate the total residual threshold uncertainty for each feature.

TABLE I. STANDARD DEVIATION OF THE SELECTED FEATURES

Units of °C	T_{sh}	T_{sc}	T_{E}	T_{D}	T_{C}	ΔT_{CA}	ΔT_{EA}
Steady-state standard deviation ($\sigma_{i,\text{SS}}$)	0.124	0.052	0.024	0.058	0.035	0.063	0.058
Standard deviation from repeatability tests ($\sigma_{i,\text{Repeat}}$)	0.101	0.156	0.084	0.280	0.166	0.088	0.111

B. *Uncertainties due to the reference models*

Since measurements are used with the reference model predictions to determine residuals, the square-root of the sum of residuals presents a non-Gaussian root-mean-square (RMS) error. Thus we analyze the no-fault measurements distribution in detail to provide the methodology for determining a proper value of the threshold ε_i. In most cases, it is hard to obtain a reference model covering all operating conditions. To train a reference model after installation, a real-time decision of fault-free or faulty status is mandatory. In contrast to the steady-state and repetition uncertainty, the model uncertainty comes from the imperfections associated with any mathematical model. We define average bias of the model estimation as the averaged residual between the model and current measurement in no zero-mean noise.

$$\sigma_{i,\mathrm{NF}}^2 = \sigma_{i,\mathrm{SS}}^2 + \sigma_{i,\mathrm{Model}}^2 \quad (3)$$

TABLE II. NET MODEL UNCERTAINTIES OF THE FEATURES USING THE 1ST, 2ND, AND 3RD ORDER MPR MODELS

Model uncertainties, $\sigma_{i,\mathrm{Model}}$ (°C)	T_{sh}	T_{sc}	T_E	T_D	T_C	ΔT_{CA}	ΔT_{EA}
1st order MPR model	0.557	0.244	0.549	0.799	0.179	0.150	0.581
2nd order MPR model	0.328	0.197	0.147	0.319	0.047	0.040	0.131
3rd order MPR model	0.197	0.133	0.123	0.250	0.029	0.019	0.071

Model standard deviation, $\sigma_{i,\mathrm{Model}}$, characterizes model uncertainty. Since zero-mean noise uncertainty ($\sigma_{i,\mathrm{SS}}$) and model uncertainties ($\sigma_{i,\mathrm{Model}}$) amplify the variability of residuals independently, it is reasonable to assume that no joint effect exists between the two uncertainties. Therefore, the covariance between the two uncertainties ($\sigma_{i,\mathrm{SS}} \cdot \sigma_{i,\mathrm{Model}}$) is zero, and $\sigma_{i,\mathrm{NF}}$ will be a squared sum of $\sigma_{i,\mathrm{SS}}$ and $\sigma_{i,\mathrm{Model}}$ as shown below. By combining the equation with Table 1, $\sigma_{i,\mathrm{Model}}$ can be estimated in Table 2. From the evaluated uncertainty, the no fault threshold is determined in section IV.

IV. Determination of No Fault Threshold

In this section, confidence intervals – the thresholds of the uncertainties evaluated in previous section – will be determined for required credibility.

A. Confidence interval, k_1, for the steady-state uncertainty

Since we use measurements and standard deviations in a preset moving window, their distribution depends on the characteristics of the moving window. When n no-fault data are sampled Gaussian with standard deviation, σ_i, the t can be defined below, where μ_i is the current mean of the moving window of n samples. In such a case, t follows a Student's t-distribution with $n-1$ degrees of freedom. When we set $1-\alpha$ probability that the two values are equal ($x_i = \mu_i$), the confidence interval, $k_1 = t_{\alpha/2,n-1}$, is described as below where $t_{\alpha/2,\,n-1}$ is a two-sided confidence interval.

$$P\left(\left| x_i - \mu_i \right| < t_{\alpha/2,n-1} \frac{\sigma_i}{\sqrt{n}} \right) = 1-\alpha \quad (6)$$

With a $1-\alpha = 99$ % confidence, $t_{0.005,9} = 3.25$ which is larger than Gaussian distribution of 2.58. Table 3 shows the values of $k_1 = t_{\alpha/2,\,9}$. For 99 % confidence (or credibility) level, k_1 is 3.25.

TABLE III. TWO-SIDED CONFIDENCE INTERVALS WITH DEGREES OF FREEDOM OF FOUR AND NINE

$1-\alpha$ (%)	80.0	90.0	95.0	99.0
$\alpha/2$ (%)	10.0	5.0	2.5	0.5
$t_{\alpha/2,4}$[1]	1.533	2.132	2.776	4.604
$k_1=t_{\alpha/2,9}$[2]	1.383	1.833	2.262	3.250

[1] 5 sample moving window
[2] 10 sample moving window

B. Confidence interval, k_2, for model uncertainty

The distribution of the T_{sh} residual using MPR model applied to the NFSS data is a Gaussian. However, residuals near zero are distributed narrower than a Gaussian. At high residual values where $|r(T_{sh})| > 1.67$°C (3.0°F), a Gaussian assumption underestimates the probability. From the Gaussian approach, 99 % of data fall within the range of ±0.6°C (±1.08°F), but no-fault test data have a wider range of ±0.78°C (±1.41°F) to cover 99 % of all data.

C. Confidence interval, k_3, for lack of measurement repeatability

Repetitive measurements of a random variable will follow a Gaussian distribution, thus, under similar measurement conditions; repetitively measured feature residuals will also follow a Gaussian distribution. Table 5 shows the confidence interval with regard to the confidence level for a Gaussian distribution at various confidence levels. For example, with 99 % credibility, k_3 equals 2.576. From the confidence intervals k_1, k_2, and k_3 obtained above, Table 5 is calculated for the feature thresholds with 50 %, 95 % and 99 % credibility for the moving window size of 10 samples.

TABLE IV. TWO-SIDED CONFIDENCE INTERVAL OF THE SEVEN FEATURES FOR THE 3RD ORDER MPR MODEL (TEMPERATURE IN °C)

$1-\alpha$ (%)		75.0	97.5	99.5
$k_2 = t_{\alpha/2,\,n-1}$	T_{sh}	1.00	2.26	2.96
	T_{sc}	0.93	2.22	3.37
	T_E	1.10	2.06	2.65
	T_D	1.15	1.96	2.63
	T_C	1.03	2.03	3.03
	ΔT_{CA}	1.14	1.95	2.64
	ΔT_{EA}	0.95	2.16	3.22

TABLE V. FEATURE THRESHOLDS AT DIFFERENT CONFIDENCE LEVELS FOR 10 SAMPLES (TEMPERATURE IN °C)

Threshold of the features	T_{sh}	T_{sc}	T_E	T_D	T_C	ΔT_{CA}	ΔT_{EA}
50 % credibility, $\varepsilon_{i,0.50}$	0.130	0.134	0.092	0.243	0.082	0.064	0.086
95 % credibility, $\varepsilon_{i,0.95}$	0.496	0.411	0.323	0.755	0.237	0.187	0.271
99 % credibility, $\varepsilon_{i,0.99}$	0.735	0.574	0.424	0.983	0.313	0.248	0.373

V. Conclusion

In this study, we developed no fault reference model of vapor compression heat pump by machine learning process with statistical evaluations. Characteristic variables were assumed to behave independently, and uncertainties were estimated in three different ways; steady-state uncertainty, repeatability uncertainty, and reference model uncertainty. From the analysis, we obtained each uncertainty and thresholds depending on the credibility. Distribution of residuals was unique compared to typical Gaussian or student t-distribution, especially larger residuals. To reduce uncertainty that may be occurred by the large residuals, it is necessary to increase threshold values to minimize false detection. From the study, a reference model of the heat pump system was obtained very handful and convenient way with an acceptable accuracy.

ACKNOWLEDGEMENTS

This paper is supported by Korea Evaluation Institute of Industrial Technology (KEIT) (No. 10063187) funded from Ministry of Trade, Industry and Energy of Republic of Korea, and authors appreciate their support.

REFERENCES

[1] J. Proctor, "Residential and small commercial central air conditioning; Rated efficiency isn't automatic," ASHRAE Winter Meeting, Jan. 26, Anaheim, CA., 2004

[2] M. S. Breuker and J. E. Braun, "Evaluating the performance of a fault detection and diagnostic system for vapor compression equipment," Int. J. of HVAC&R Research, vol. 4, no. 4, pp. 401-425, 1998.

[3] T. M. Rossi, "Detection, diagnosis, and evaluation of faults in vapor compression cycle equipment," Ph.D. Dissertation, Purdue Univ., West Lafayette, IN, USA, 1995.

[4] A. S. Glass, P. Gruber, M. Roos, and J. Tödtli, "Qualitative model-based fault detection in air-handling units," IEEE Control Systems Magazine, vol. 15, no. 4, pp. 11-22, 1995.

[5] H. Li, "A decoupling-based unified fault detection and diagnosis approach for packaged air conditioners," Ph.D. Dissertation, Purdue Univ., West Lafayette, IN, USA, 2004.

[6] M. Kim, W. V. Payne, P. A. Domanski, and C. J. L. Hermes, "Performance of a residential heat pump operating in the cooling mode with single faults imposed," NISTIR 7350, National Institute of Standards and Technology, Gaithersburg, MD, USA, 2006.

 ISBN: 978-1-61208-576-0